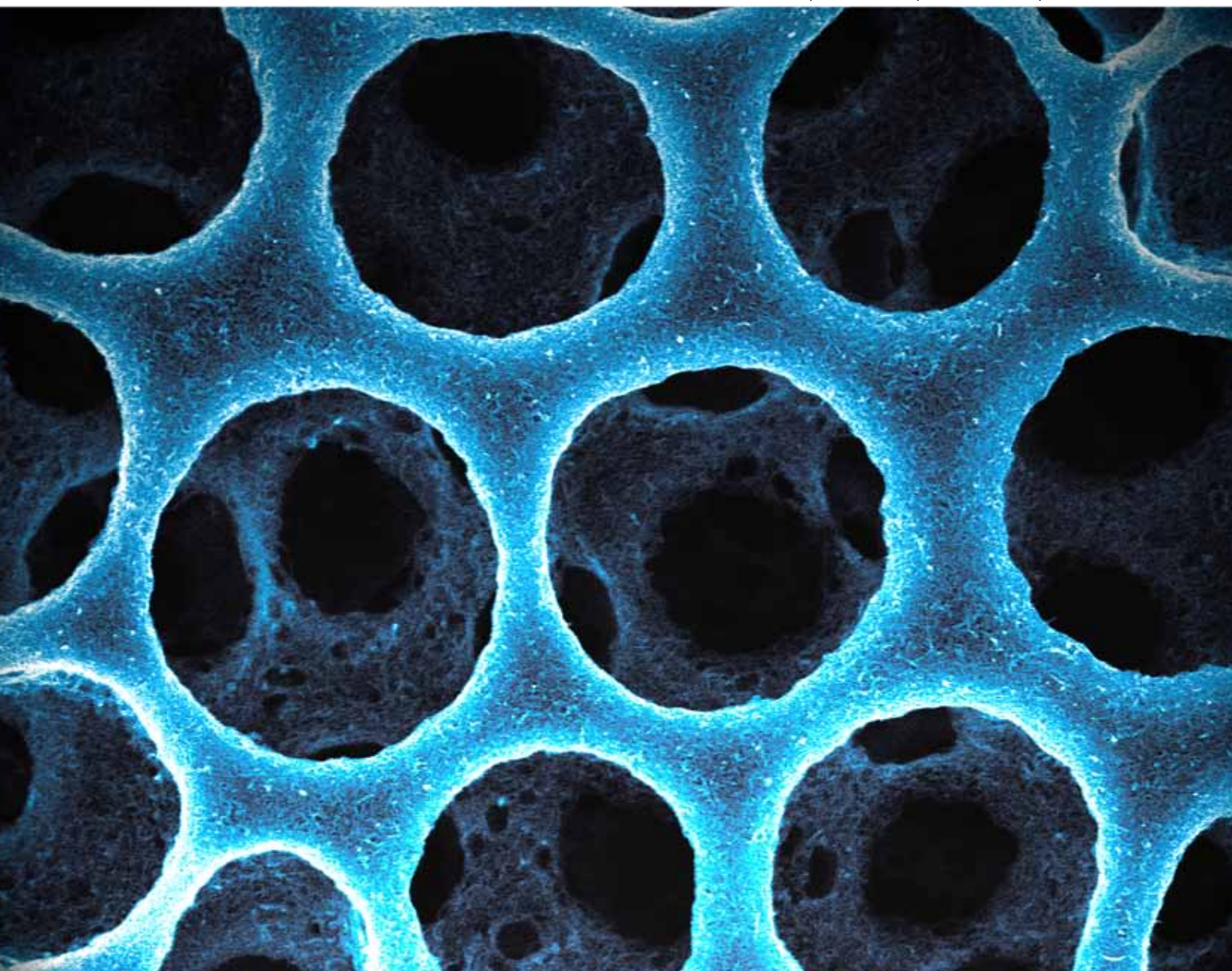


Soft Matter

www.softmatter.org

Volume 5 | Number 12 | 21 June 2009 | Pages 2325–2480



Emerging Investigators

ISSN 1744-683X

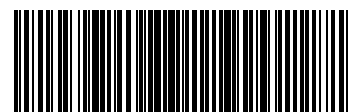
RSC Publishing

COMMUNICATION

Sang Ouk Kim *et al.*
Highly entangled carbon nanotube
scaffolds by self-organized aqueous
droplets

PAPER

Fernando Bresme *et al.*
Heat transfer in soft nanoscale
interfaces: the influence of interface
curvature



1744-683X(2009)5:12;1-4

Highly entangled carbon nanotube scaffolds by self-organized aqueous droplets†‡

Sun Hwa Lee, Ji Sun Park, Bo Kyung Lim, Chan Bin Mo, Won Jun Lee, Ju Min Lee, Soon Hyung Hong and Sang Ouk Kim*

Received 6th October 2008, Accepted 20th November 2008

First published as an Advance Article on the web 3rd December 2008

DOI: 10.1039/b817477f

We present a facile and versatile directed assembly process for highly entangled carbon nanotube (CNT) scaffolds. Macroporous polymer/CNT nanocomposites were prepared by a ‘breath figure’ method. After pyrolysis of the nanocomposites, highly stable CNT scaffolds with diverse morphologies such as monolayered or multi-layered cellular films or individual CNT rings were prepared. The cellular CNT scaffolds demonstrated high electrical conductivity and field-emission properties, which is potentially useful for various applications in electronics and energy storage devices.

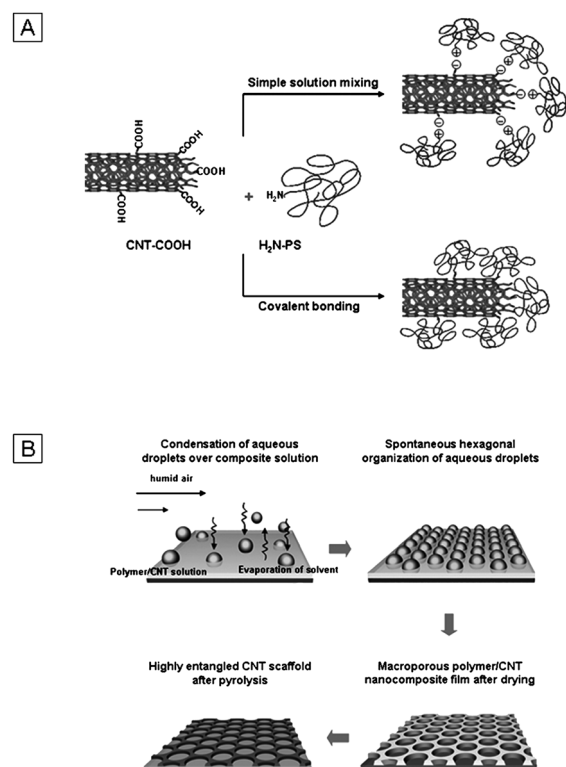
The organization of nanoscale building blocks into a desired architecture is currently a challenging subject in materials science. It is critical to direct the macroscopic-scale as well as the molecular-scale arrangement of nanoscale building blocks for various functional nanomaterials.¹ In particular, the organization of carbon nanotubes (CNTs) into films,² fibers,³ gels⁴ or micropatterned materials⁵ may provide versatile opportunities for applications in nanoelectronics,⁶ energy storage devices,⁷ sensors,⁸ bioscaffolds,⁹ *etc.* To date, the organization process for CNTs has been mostly developed in conjunction with the CNT growth process.¹⁰ The process of controlled growth and organization may generate well-defined CNT architectures with various useful morphologies. However, combining large-scale CNT growth with organization processes requires complicated facilities and multiple steps.

Self-assembly is an alternative approach to organizing nanomaterials into a functional architecture. Since self-assembly relies on the spontaneous and parallel organization of pre-existing building blocks, it is cost-effective as well as beneficial for large-scale organization processes.^{1,11} Furthermore, it can be universally applied to diverse nanomaterials without any severe chemical or thermal damage to them. The previously developed self-assembly processes for CNTs have applied selective wetting on prepatterned surfaces¹² or spontaneous alignment under external fields,¹³ and have mainly focused on directing the orientational ordering of individual nanotubes.

Here we present a facile and versatile directed assembly method to produce cellular CNT scaffolds with tunable morphologies. Cellular

films or mats consisting of highly entangled CNTs were fabricated by a self-organized micropatterning process followed by pyrolysis. The self-organization of aqueous droplets upon a volatile solution, generally known as a ‘breath figure’,¹⁴ has been applied to an organic solution containing both polymer and CNTs as solutes and has yielded macroporous polymer/CNT nanocomposite films. Upon the calcination of the polymer matrices, the resultant highly entangled CNT scaffolds retained the macroporous morphology. Owing to the simple process and morphological diversity, the CNT scaffolds are anticipated to be useful for various applications. In this work, their electric conductivity and field-emission properties have been explored to elucidate potential applications for nanoelectronics and energy storage materials.

The procedure for creating the CNT scaffold is schematically depicted in Scheme 1. The precursor solution, which included homogeneously dispersed multi-walled carbon nanotubes



Scheme 1 Schematics for (A) covalent vs. noncovalent CNT functionalization methods and (B) the directed assembly process for preparing CNT scaffolds.

Department of Materials Science and Engineering, KAIST, Daejeon, 305-701, Republic of Korea. E-mail: sangouk.kim@kaist.ac.kr; Fax: +82 42 350 3310; Tel: +82 42 350 3339

† This paper is part of a *Soft Matter* issue highlighting the work of emerging investigators in the soft matter field.

‡ Electronic supplementary information (ESI) available: Experimental details and additional SEM images of cellular CNT scaffolds. See DOI: 10.1039/b817477f

(MWNTs), was prepared by dissolving predetermined amounts of purified MWNTs and amine-terminated polystyrene (PS-NH₂) (MW 3000 g mol⁻¹) in benzene. As shown in Scheme 1A, the PS-NH₂ was covalently or noncovalently grafted to the defect sites of the purified MWNTs, enabling the homogenous dispersion of the MWNTs in the organic medium. The detailed procedure and characterization of covalent and noncovalent functionalization methods have been published elsewhere.^{15,16} As illustrated in Scheme 1B, the precursor solution was deposited upon a substrate under a stream of humid air. The endothermic evaporation of volatile benzene cooled down the solution surface, upon which aqueous droplets condensed from the humid air. The condensed droplets were stabilized by thermocapillary convection, and the elastic interaction among them led to hexagonal packing.¹⁷ At this stage, the nucleation and growth of aqueous droplets confined CNTs in the capillary surrounding the aqueous droplets and created the highly-entangled morphologies of the CNT scaffolds. After the complete drying of benzene and water, a porous PS/CNT nanocomposite film remained upon the substrate. The subsequent pyrolysis of the polymer matrix at high temperature revealed the highly entangled CNT framework inside the composite film. Owing to the fine dispersion of the functionalized carbon nanotubes and the geometrical confinement imposed by aqueous droplets, highly stabilized CNT scaffolds with diverse morphologies, such as multilayered porous mats, monolayered cellular films, and individually separated rings, were created.

Fig. 1 shows scanning electron microscopy (SEM) images of the monolayered cellular films before and after pyrolysis. The plane-view of the nanocomposite film (Fig. 1A) shows a porous morphology with a pore diameter on the micrometre scale. The precursor solution included 3 mg ml⁻¹ of PS-NH₂ and 1 mg ml⁻¹ of MWNTs. Note that when micrometre-length CNT strands are included in a nanocomposite film, the size uniformity and regular packing of macropores deteriorates to a moderate extent.^{14c} As presented in the cross-sectional view of the fractured films (Fig. 1B), the noncovalent grafting through zwitterionic interaction yielded a homogeneous dispersion of CNTs in the polymer matrix. (C) Plane-view of the highly entangled CNT scaffold after pyrolysis of the polymer matrix. (D) 60° tilted SEM image of the fractured CNT scaffold. CNT scaffold maintains its three-dimensional scaffold structure.

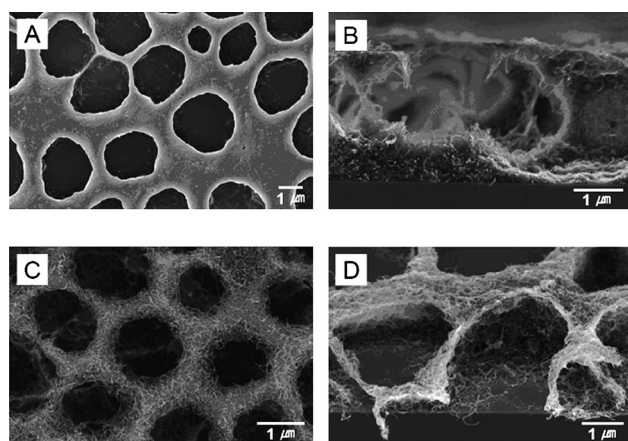


Fig. 1 SEM images of monolayered cellular scaffolds before and after pyrolysis. (A) Plane-view of the porous PS/CNT nanocomposite film. (B) Cross-sectional image of the PS/CNT nanocomposite film. CNTs are well-dispersed in the polymer matrix. (C) Plane-view of the highly entangled CNT scaffold after pyrolysis of the polymer matrix. (D) 60° tilted SEM image of the fractured CNT scaffold. CNT scaffold maintains its three-dimensional scaffold structure.

benzene, the aqueous droplets condensed upon the precursor solution sank down to the underlying hard substrate (Si wafer) during the film preparation, such that the resultant macropores penetrated throughout the film thickness. Although the film thickness decreased from 2.8 μm to 1.2 μm during the calcination of the polymer matrix, the CNT scaffold preserved the porous morphology of the nanocomposite film. As shown in Fig. 1C, CNTs were highly entangled in the scaffold, which provided the mechanical stability required to endure the severe calcination process.

The 60° tilted SEM image of the fractured sample (Fig. 1D) clearly demonstrates that the scaffold maintained its three-dimensional structure without any polymer matrix. We note that the CNT scaffolds prepared from uniform nanocomposite films did not show sufficient mechanical stability to endure the thermal calcination process. When a drop of nanocomposite solution was dried under a stream of dry nitrogen gas and subsequently calcined, the remaining CNT scaffold collapsed (see ESI Fig. S1†). This demonstrates that the geometric confinement imposed by growing aqueous droplets plays a significant role in enhancing CNT entanglement and stabilizing the three-dimensional architecture of a scaffold.

The self-organized morphology of CNT scaffolds could be varied by changing the CNT and PS-NH₂ concentration in the precursor solution. When the concentration was sufficiently high, the multilayered porous morphology was produced (see Fig. 2 & ESI Fig. S2). The porous mats shown in Fig. 2A and 2B were fabricated from a precursor solution containing 10 mg ml⁻¹ of PS-NH₂ and 1 mg ml⁻¹ of MWNTs. The cross-sectional SEM image (Fig. 2B) clearly reveals the three layers of macroporous CNT membranes. The MWNTs were tightly entangled, enclosing the mutually connected pores. When the concentration of PS-NH₂ and MWNTs in the precursor solution was reduced to 0.5 mg ml⁻¹ and 0.1 mg ml⁻¹, respectively,

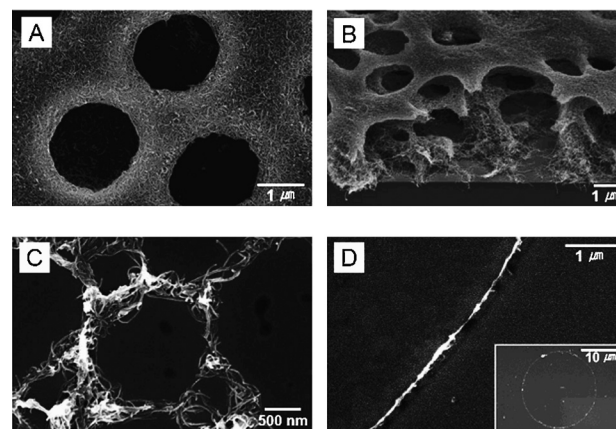


Fig. 2 SEM images showing various morphologies of CNT scaffolds according to the CNT functionalization method and concentrations of polymer/CNTs. (A, B) Plane and cross-sectional views of the multilayered porous CNT mat prepared from a precursor solution including 10 mg ml⁻¹ of PS-NH₂ and 1 mg ml⁻¹ of MWNTs. The CNT mat consisted of three-layered macroporous structure. (C) Magnified image of a monolayered cellular scaffold showing CNTs woven into the hexatic thin strands. The precursor solution contained 0.5 mg ml⁻¹ of PS-NH₂ and 0.1 mg ml⁻¹ of MWNTs. (D) Magnified image of a CNT ring scaffold fabricated from covalently functionalized CNTs (PS-CNT). The inset shows the overall ring structure. The concentration of PS-CNT was 0.05 mg ml⁻¹ in benzene.

monolayered cellular films were created. Fig. 2C shows a magnified image of a thin cellular network whose framework consists of several strands of highly entangled CNTs. The morphology of the CNT scaffold transformed into individually separated rings when the covalently functionalized CNTs (CNT-PS) were used. Fig. 2D shows the ring pattern prepared from the solution containing 0.05 mg ml^{-1} of CNT-PS. Without any excess free polymeric molecules in the precursor solution, the breath figure morphology was poorly stabilized, such that individually separated rings of entangled CNTs were left on the substrates.¹⁸

The surface electric resistance was measured by a four-point probe method to confirm the electrical conductivity of the CNT scaffold. The surface resistance of the nanocomposite film prepared from a precursor solution including 5 mg ml^{-1} of PS-NH₂ and 1 mg ml^{-1} of MWNTs, was $1.37 \times 10^5 \Omega/\text{square}$ before the removal of the polymer matrix. However, after calcination, the surface resistance dramatically decreased to $4.3 \times 10^3 \Omega/\text{square}$, a decrease of about 10^2 -fold compared to the value of the composite. This indicates that the electrical properties of the CNTs were well preserved during the severe calcination process and, furthermore, that the CNTs were sufficiently connected to provide the electro-conductive path.

Among the diverse and useful properties of porous CNT films, the field-emission properties have been measured based on a diode-type structure at room temperature in a high-vacuum chamber.¹⁹ Fig. 3A shows an SEM image of CNT field emitters after calcination. The CNTs are standing upright on ITO glass and some of them are protruding from the entangled scaffold. These protruding CNTs could act as electron emitters under the influence of an applied voltage. Fig. 3B presents the emission current density against applied electric field. The turn-on field was $1.79 \text{ V } \mu\text{m}^{-1}$ at an emission current density of $10 \mu\text{A cm}^{-2}$, and the current density was $450 \mu\text{A cm}^{-2}$ at an electric field of $2.8 \text{ V } \mu\text{m}^{-1}$. These values are comparable with that of CNT field emitters grown by CVD^{20,21} or single-walled carbon nanotube emitters.²² The excellent field-emission properties of the

CNT scaffold is attributed to the large number of CNT emitters and adequate spacing between them which avoids a screening effect.^{21,23} The Fowler–Nordheim plot in Fig. 3C demonstrates the typical field-emission behavior of CNT emitters.¹⁹

In summary, we have demonstrated a novel strategy to fabricate highly entangled, cellular CNT scaffolds. The simple processing through self-organized micropatterning and pyrolysis produced CNT scaffolds with diverse morphologies such as monolayered cellular films, multilayered mats, and rings. Our approach represents considerable progress toward the low-cost, large-scale engineering of CNT assemblies. The resultant highly entangled CNT scaffolds had a high electrical conductivity. Furthermore, they showed excellent field-emission properties owing to their unique architectures. These electro-conductive, highly entangled scaffolds with large surface areas are potentially advantageous for numerous applications. Representative examples are electrode materials for energy conversion/storage devices such as solar cells, fuel cells, and supercapacitors, or supporting frameworks for catalyst particles.

Acknowledgements

This work was supported by the second stage of the Brain Korea 21 Project, National Research Laboratory Program (R0A-2008-000-20057-0), the 21st Century Frontier Research Program (Center for Nanoscale Mechatronics and Manufacturing, 08K1401-01010), and the Fundamental R&D Program for Core Technology of Materials funded by the Korean government.

References

- (a) C. M. Niemeyer and C. A. Mirkin, *Nanobiotechnology*, Wiley-VCH, Weinheim, 2004; (b) R. W. Kelsall, I. W. Hamley and M. John. Geoghegan, *Nanoscale Science and Technology*, Wiley & Sons, Chichester, 2005; (c) Y. Huang, X. Duan, Q. Wei and C. M. Lieber, *Science*, 2001, **291**, 630; (d) S. O. Kim, H. H. Solak, M. P. Stoykovich, N. J. Ferrier, J. J. de Pablo and P. F. Nealey, *Nature*, 2003, **424**, 411; (e) T. H. Han, J. Kim, J. S. Park, H. Ihee and S. O. Kim, *Adv. Mater.*, 2007, **19**, 3924; (f) S. O. Kim, B. H. Kim, D. Meng, D. O. Shin, C. M. Koo, H. H. Solak and Q. Wang, *Adv. Mater.*, 2007, **19**, 3271; (g) B. H. Kim, D. O. Shin, S.-J. Jeong, C. M. Koo, S. C. Jeon, W. J. Hwang, S. Lee, M. G. Lee and S. O. Kim, *Adv. Mater.*, 2008, **20**, 2303.
- (a) Z. Wu, Z. Chen, X. Du, J. M. Logan, J. Sippel, M. Nikolou, K. Kamaras, J. R. Reynolds, D. B. Tanner, A. F. Hebard and A. G. Rinzler, *Science*, 2004, **305**, 1273; (b) M. Zhang, S. Fang, A. A. Zakhidov, S. B. Lee, A. E. Aliev, C. D. Williams, K. R. Atkinson and R. H. Baughman, *Science*, 2005, **309**, 1215.
- (a) Y.-L. Li, I. A. Kinloch and I. A. H. Windle, *Science*, 2004, **304**, 276; (b) A. B. Dalton, S. Collins, E. Muñoz, J. M. Razal, V. H. Ebron, J. P. Ferraris, J. N. Coleman, B. G. Kim and R. H. Baughman, *Nature*, 2003, **423**, 703; (c) L. M. Ericson, H. Fan, H. Peng, V. A. Davis, W. Zhou, J. Sulpizio, Y. Wang, R. Booker, J. Vavro, C. Guthy, A. N. G. Parra-Vasquez, M. J. Kim, S. Ramesh, R. K. Saini, C. Kittrell, G. Lavin, H. Schmidt, W. W. Adams, W. E. Billups, M. Pasquali, W.-F. Hwang, R. H. Hauge, J. E. Fischer and R. E. Smalley, *Science*, 2004, **305**, 1447.
- (a) T. Fukushima, A. Kosaka, Y. Ishimura, T. Yamamoto, T. Takigawa, N. Ishii and T. Aida, *Science*, 2003, **300**, 2072; (b) M. B. Bryning, D. E. Milkie, M. F. Islam, L. A. Hough, J. M. Kikkawa and A. G. Yodh, *Adv. Mater.*, 2007, **19**, 661.
- (a) M. Lee, B. Y. Lee, S. Myung, J. Kang, L. Huang, Y.-K. Kwon and S. Hong, *Nat. Nanotechnol.*, 2006, **1**, 66; (b) N. Chakrapani, B. Wei, A. Carrillo, P. M. Ajayan and R. S. Kane, *Proc. Natl. Acad. Sci. U. S. A.*, 2004, **101**, 4009.

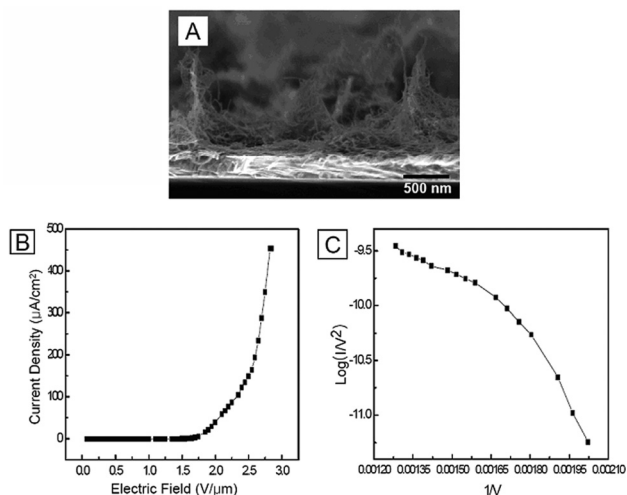


Fig. 3 (A) SEM image of CNT field emitter after calcination. CNTs protrude from entangled CNT scaffold which was prepared from a precursor solution including 2 mg ml^{-1} of PS-NH₂ and 1 mg ml^{-1} MWNTs. (B) The plot of emission current density of cellular CNT films versus applied electrical field. The turn-on field is $1.79 \text{ V } \mu\text{m}^{-1}$ at the current density of $10 \mu\text{A cm}^{-2}$ (C) The Fowler–Nordheim plot representing the conventional field-emission behavior of CNT emitters.

- 6 (a) M. Ouyang, J.-L. Huang, C. L. Cheung and C. M. Lieber, *Science*, 2001, **291**, 97; (b) P. G. Collins, A. Zettl, H. Bando, A. Thess and R. E. Smalley, *Science*, 1997, **278**, 100.
- 7 (a) R. H. Baughman, A. A. Zakhidov and W. A. de Heer, *Science*, 2002, **297**, 787; (b) G. Che, B. B. Lakshmi, E. R. Fisher and C. R. Martin, *Nature*, 1998, **393**, 346.
- 8 (a) J. Kong, N. R. Franklin, C. Zhou, M. G. Chapline, S. Peng, K. Cho and H. Dai, *Science*, 2000, **287**, 622; (b) A. Modi, N. Koratkar, E. Lass, B. Wei and P. M. Ajayan, *Nature*, 2003, **424**, 171.
- 9 (a) M. A. Correa-Duarte, N. Wagner, J. Rojas-Chapana, C. Morszeck, M. Thie and M. Giersig, *Nano Lett.*, 2004, **4**, 2233; (b) A. R. Boccaccini, F. Chicatun, J. Cho, O. Bretcanu, J. A. Roether, S. Novak and Q. Chen, *Adv. Funct. Mater.*, 2007, **17**, 2815.
- 10 (a) S. J. Kang, C. Kocabas, T. Ozel, M. Shim, N. Pimparkar, M. A. Alam, S. V. Rotkin and J. A. Rogers, *Nat. Nanotechnol.*, 2007, **2**, 230; (b) D. N. Futaba, K. Hata, T. Yamada, T. Hiraoka, Y. Hayamizu, Y. Kakudate, O. Tanaike, H. Hatori, M. Yumura and S. Iijima, *Nat. Mater.*, 2006, **5**, 987; (c) B. Q. Wei, R. Vajtai, Y. Jung, J. Ward, R. Zhang, G. Ramanath and P. M. Ajayan, *Nature*, 2002, **416**, 495; (d) D. H. Lee, D. O. Shin, W. J. Lee and S. O. Kim, *Adv. Mater.*, 2008, **20**, 2480.
- 11 (a) G. M. Whitesides and B. Grzybowski, *Science*, 2002, **295**, 2418; (b) G. M. Whitesides and M. Boncheva, *Proc. Natl. Acad. Sci. U. S. A.*, 2002, **99**, 69.
- 12 (a) Y. Wang, D. Maspoeh, S. Zou, G. C. Schatz, R. E. Smalley and C. A. Mirkin, *Proc. Natl. Acad. Sci. U. S. A.*, 2006, **103**, 2026; (b) S. G. Rao, L. Huang, W. Setyawan and S. Hong, *Nature*, 2003, **425**, 36.
- 13 (a) M. R. Diehl, S. N. Yaliraki, R. A. Beckman, M. Barahona and J. R. Heath, *Angew. Chem., Int. Ed.*, 2002, **41**, 353; (b) G. Yu, A. Cao and C. M. Lieber, *Nat. Nanotechnol.*, 2007, **2**, 372; (c) R. Sharma, C. Y. Lee, J. H. Choi, K. Chen, M. S. Strano and M.S., *Nano Lett.*, 2007, **7**, 2693.
- 14 (a) G. Widawski, M. Rawiso and B. François, *Nature*, 1994, **369**, 387; (b) H. Yabu and M. Shimomura, *Chem. Mater.*, 2005, **17**, 5231; (c) J. S. Park, S. H. Lee, T. H. Han and S. O. Kim, *Adv. Funct. Mater.*, 2007, **17**, 2315; (d) H. T. Ham, I. J. Chung, Y. S. Choi, S. H. Lee and S. O. Kim, *J. Phys. Chem. B*, 2006, **110**, 13959; (e) S. H. Lee, H. T. Ham, J. S. Park, I. J. Chung and S. O. Kim, *Macromol. Symp.*, 2007, **249–250**, 618; (f) H. Takamori, T. Fujigaya, Y. Yamaguchi and N. Nakashima, *Adv. Mater.*, 2007, **19**, 2535; (g) A. Böker, Y. Lin, K. Chiapperini, R. Horowitz, M. Thompson, V. Carreon, T. Xu, C. Abetz, H. Skaff, A. D. Dinsmore, T. Emrick and T. P. Russell, *Nat. Mater.*, 2004, **3**, 302.
- 15 (a) J. Chen, M. A. Hamon, H. Hu, Y. Chen, A. M. Rao, P. C. Eklund and R. C. Haddon, *Science*, 1998, **282**, 95; (b) H. T. Ham, C. M. Koo, S. O. Kim, Y. S. Choi and I. J. Chung, *Macromol. Res.*, 2004, **12**, 384.
- 16 (a) M. A. Hamon, J. Chen, H. Hu, Y. Chen, M. E. Itkis, A. M. Rao, P. C. Eklund and R. C. Haddon, *Adv. Mater.*, 1999, **11**, 834; (b) S. H. Lee, J. S. Park, C. M. Koo, B. K. Lim and S. O. Kim, *Macromol. Res.*, 2008, **16**, 261; (c) S. H. Lee, J. S. Park, B. K. Lim and S. O. Kim, *J. Appl. Polym. Sci.*, 2008, **110**, 2345.
- 17 (a) M. Srinivasarao, D. Collings, A. Philips and S. Patel, *Science*, 2001, **292**, 79; (b) U. H. F. Bunz, *Adv. Mater.*, 2006, **18**, 973.
- 18 B. P. Khanal and E. R. Zubarev, *Angew. Chem., Int. Ed.*, 2007, **46**, 2195.
- 19 S. I. Cha, K. T. Kim, S. N. Arshad, C. B. Mo, K. H. Lee and S. H. Hong, *Adv. Mater.*, 2006, **18**, 553.
- 20 S. Fan, M. G. Chapline, N. R. Franklin, T. W. Tomblor, A. M. Cassell and H. Dai, *Science*, 1999, **283**, 512.
- 21 L. Nilsson, O. Groening, C. Emmenegger, O. Kuettel, E. Schaller, L. Schlappbach, H. Kind, J.-M. Bonard and K. Kern, *Appl. Phys. Lett.*, 2000, **76**, 2071.
- 22 (a) J.-M. Bonard, J.-P. Salvetat, T. Stöckli, W. A. de Heer, L. Forró and A. Châtelain, *Appl. Phys. Lett.*, 1998, **73**, 918; (b) J. E. Jung, Y. W. Jin, J. H. Choi, Y. J. Park, T. Y. Ko, D. S. Chung, J. W. Kim, J. E. Jang, S. N. Cha, W. K. Yi, S. H. Cho, M. J. Yoon, C. G. Lee, J. H. You, N. S. Lee, J. B. Yoo and J. M. Kim, *Physica B*, 2002, **323**, 71; (c) N. S. Lee, D. S. Chung, I. T. Han, J. H. Kang, Y. S. Choi, H. Y. Kim, S. H. Park, Y. W. Jin, W. K. Yi, M. J. Yun, J. E. Jung, C. J. Lee, J. H. You, S. H. Jo, C. G. Lee and J. M. Kim, *Diamond Relat. Mater.*, 2001, **10**, 265.
- 23 J. S. Suh, K. S. Jeong, J. S. Lee and I. Han, *Appl. Phys. Lett.*, 2002, **80**, 2392.